Brownian oscillations in colloidal systems studied by Mossbauer spectroscopy

1992 J. Phys.: Condens. Matter 4 3109

(http://iopscience.iop.org/0953-8984/4/12/009)

J. Phys.: Condens. Matter 3 (1991) 3109–3124. Printed in the UK

Brownian oscillations in colloidal systems studied by Mössbauer spectroscopy

P V Hendriksen, S Mørup and S Linderoth

Laboratory of Applied Physics, Technical University of Denmark, DK-2800 Lyngby, Denmark

Received 17 September 1991, in final form 28 November 1991

Abstract. By means of Mössbauer spectroscopy we have studied the dynamics of nano-sized particles when these are dispersed in decalin in the form of a crystalline matrix or as a supercooled liquid. In the case of a crystalline matrix the particles perform Brownian oscillations at temperatures close to the melting point of the decalin. In the case of a supercooled liquid ordinary Brownian motion is observed.

1. Introduction

The sensitivity of the line shape of the Mössbauer spectrum on atomic diffusion was predicted in 1960 by Singwi and Sjölander [1]. Since then Mössbauer spectroscopy has proven to be a valuable tool in the study of atomic diffusion in solids [2] and for the study of molecular motion in liquids [3]. The method has also successfully been applied in the study of Brownian motion [4] and protein dynamics [5, 6].

The mean lifetime of the decaying nucleus ($\tau_N = 141$ ns for ^{57}Fe) is a characteristic time of the Mössbauer experiment; motions with correlation times on this timescale (10^{-7}–10^{-9} s) may influence the line shape of the spectrum [5, 7]. If the correlation times are much shorter, only the area of the spectrum will be affected [5, 7]. The area of the Mössbauer spectrum is proportional to the fraction (f) of absorption events that take place without recoil of the nucleus. This fraction can be expressed in terms of the mean-square displacement $\langle x^2 \rangle$ of the nucleus [7]:

$$f = \exp(-k^2\langle x^2 \rangle) \tag{1}$$

where $k = 2\pi/\lambda$ is the wavenumber and λ (= 0.086 nm for ^{57}Fe) is the wavelength of the γ-ray.

The Brownian motion of particles suspended in a viscous liquid has a timescale such that the motion may influence the line shape of the Mössbauer absorption line. Theory predicts a mere broadening of the absorption line proportional to the diffusion constant of the particles in the liquid [1]. This has been found experimentally in several cases, for instance for 165 Å magnetite particles in glycerol [8], for 100 Å magnetite particles in a diester carrier [9], and for 650 Å SnO_2 particles in glycerol [10]. Discrepancies with the picture that diffusion just causes a broadening of the absorption line without altering the Lorentzian line shape, have also been reported [4, 11, 12]. The experimental work in this field has been reviewed by Bhide *et*

0953-8984/91/123109+16$03.50

al [4], who also elaborate further on the theory of how Brownian motion influences the Mössbauer spectrum.

In the study of the dynamics of proteins [5] and other biological systems [6, 13], it has been found that the line shape of the spectrum changes with temperature. Above a certain temperature the spectrum appears to be a sum of narrow and broad Lorentzians [5, 6]. This is typical of diffusive motion restricted in space [3], and the results are generally interpreted in terms of a model of overdamped harmonic oscillators in Brownian motion—called Brownian oscillations [14].

The co-existence of narrow and broad components in the Mössbauer spectrum, induced by the dynamics of the nuclei, has also been reported for other systems. In a study of the motion of nano-sized particles caged in a polymeric network, Plachinda and co-workers [15, 16] observed this effect, and Hayashi *et al* [17] reported similar findings in a study of loosely packed sinters of copper and silver powders, applying ^{197}Au Mössbauer spectroscopy.

Recently Parak *et al* [18] have repeated one of the classical experiments in the study of atomic diffusion, namely the study of ^{57}Fe(II) diffusion in glycerol. Contrary to earlier measurements [19–21] they found that in order to explain the variation of line shape with temperature one needs more than one Lorentzian. They pointed out that, as seen by Mössbauer spectroscopy, the atomic motion of ^{57}Fe(II) in a glycerol glass seems to be very similar to motion of the iron atoms in myoglobia molecules.

In this paper we report on investigations of the motion of iron particles when these are dispersed in a crystalline matrix or a supercooled liquid. In the case of a crystalline matrix the changes of the Mössbauer spectrum induced by particle motion are very similar to those reported for biological systems and for polymeric-bound particles. These Mössbauer spectra are analysed by using the model of Brownian oscillations. In the case of a supercooled liquid a broadening of the absorption lines, with no changes of the Lorentzian line shapes, is observed. This is interpreted as being caused by particle diffusion, and we therefore analyse the spectra on the basis of the model by Singwi and Sjölander [1].

2. Theory

The absorption cross section, $\sigma_a(\omega)$, for a γ-quantum with energy $E = \hbar\omega$ can be written as the time and space Fourier transform of the time-dependent self-correlation function, $G_s(r, t)$ [1, 3, 22]

$$\sigma_a(\omega) = \frac{\sigma_0}{4\tau_N} \int\int \exp\left\{ i[k \cdot r - (\omega - \omega_0)t] - \frac{t}{2\tau_N} \right\} G_s(r, t)\, dr\, dt \quad (2)$$

The self-correlation function, $G_s(r, t)$, expresses the dynamics of the absorbing nuclei. In the classical limit $G_s(r, t)$ is the probability of finding the nucleus at the position r if it was at the origo at $t = 0$. σ_0 is the resonance absorption cross section, τ_N is the mean lifetime of the excited state, k is the wavevector of the γ-ray and $\hbar\omega_0$ is the energy of the excited nuclear state. Inserting the self-correlation function for a given mode of motion into equation (2), and folding the resulting cross section for γ-ray absorption with the energy profile of the γ-ray emitted from the source, yields the Mössbauer spectrum.

2.1. Brownian oscillations

To explain the characteristic changes in the Mössbauer spectrum of proteins a model of Brownian motion in a harmonic potential has been suggested [6, 23]. The motion is 'driven' by the random force $F(t)$, and the particle is further acted upon by a harmonic force $(-m\Omega^2 r)$ and by a frictional force $(-m\beta\dot{r})$. The equation of motion becomes

$$m\ddot{r} + m\beta\dot{r} + m\Omega^2 r = F(t) \tag{3}$$

where $m\Omega^2$ is the harmonic force constant, β is the frictional force constant and m the mass of the particle. This type of motion has both an oscillatory and a diffusive nature. The correlation function of the motion is known in the overdamped case ($\beta \gg \Omega$), and the Mössbauer spectrum can in this limit be written [13]

$$I(\omega) = \frac{1}{2\pi}\int_{-\infty}^{\infty} \exp\left[-i(\omega-\omega_0)t - \frac{1}{2}\Gamma|t| - k^2\langle x_{BO}^2\rangle(1-e^{-\alpha|t|})\right] \tag{4}$$

where $\Gamma = 1/\tau_N$ is the natural line width (in units of s^{-1}), and $\alpha = \Omega^2/\beta$ is the ratio between the harmonic force and the damping. $\langle x_{BO}^2\rangle$ is the mean-square displacement of the nuclei caused by the Brownian oscillations. If the exponential $\exp(-k^2\langle x_{BO}^2\rangle e^{-\alpha t})$ is expanded in a power series the Mössbauer spectrum can be expressed as an infinite sum of Lorentzians [13, 23],

$$I(\omega) = e^{-k^2\langle x_{BO}^2\rangle}\sum_{n=0}^{\infty}\frac{(k^2\langle x_{BO}^2\rangle)^n}{n!}\frac{(\frac{1}{2}\Gamma + n\alpha)/\pi}{(\frac{1}{2}\Gamma + n\alpha)^2 + (\omega-\omega_0)^2}. \tag{5}$$

The first Lorentzian in the expansion ($n = 0$) has the natural line width (Γ). The action of the Brownian oscillations is to shift the area from this component to the quasi-elastic broader components. The weight of each of the broad components is given by the factor $(k^2\langle x_{BO}^2\rangle)^n/n!$.

The lattice vibrations (v) within the particles will also contribute to the total mean-square displacement of the nuclei. Assuming the lattice vibrations to be uncorrelated with the Brownian oscillations the total mean-square displacement will be

$$\langle x_{tot}^2\rangle = \langle x_{BO}^2\rangle + \langle x_v^2\rangle. \tag{6}$$

3. Experimental procedure

The investigated samples were prepared by thermal decomposition of iron pentacarbonyl in decalin in the presence of surfactants (oleic acid or Sarkosyl-O). This process is described in detail elsewhere [24–26]. The process results in the formation of a stable suspension of amorphous iron–carbon particles containing about 25 at% carbon [27–29]. The mean particle size can be controlled by, e.g., the choice of surfactant [25, 26]. The particles have a very narrow size distribution [25, 28, 29], which makes this a good model system for experimental studies of the fundamental properties of small particles. Previous studies of particle dynamics in ferrofluids [8, 9] have been faced with the problem of very broad particle size distributions.

One sample (A) was frozen in liquid nitrogen immediately after the preparation, and was kept under liquid nitrogen until the time of measurement. Another sample (B) was exposed to air for about one month. This resulted in evaporation of the decalin and oxidation of the particles. The oxidized particles were then re-suspended in decalin, and cooled to liquid nitrogen temperature.

Mössbauer investigations have been performed by using a constant-acceleration spectrometer with a 50 mCi source of ^{57}Co in rhodium. The spectrometer was calibrated with a 12.5 μm α-iron foil at room temperature. Isomer shifts are given relative to the centroid of this spectrum. Measurements at 12 K were performed with the samples attached to the cold finger of a closed-cycle He refrigerator. Measurements between 80 and 295 K were made with the samples mounted in a liquid-nitrogen cryostat. The temperature was controlled with a stability better than ± 0.5 K. The temperature was measured with a copper–constantan thermocouple. Mössbauer spectra have been obtained in velocity intervals of ± 12 mm s^{-1}, ± 24 mm s^{-1}, and in a few cases up to ± 80 mm s^{-1}.

In order to characterize the state of the carrier medium the samples were investigated by x-ray diffraction and differential thermal analysis (DTA). Care was taken that the thermal history of the sample was the same no matter which technique was applied.

Particle sizes have been determined from electron micrographs (Phillips EM 430) and by Mössbauer spectroscopy [29].

Measurements on two samples (A and B) are presented in the following. Key features of these are presented in table 1.

Table 1. Composition and particle size of the samples.

Sample	Particles	Mean size (d)	Standard deviation	Surfactant
A	Fe–C	3.3 nm	0.3 nm	Oleic acid
B	Iron oxide	6.8 nm	0.7 nm	Sarkosyl-O

4. Results

4.1. Sample A

Figure 1 shows the 12 K spectrum of sample A. The spectrum is a superposition of a magnetically split component with very broad lines ($\langle B \rangle = 27$ T) and a quadrupole doublet. The magnetically split component has previously [27, 29] been identified as amorphous $Fe_{1-x}C_x$ with $x \approx 25\%$ [29]. The quadrupole doublet ($\Delta E_Q = 2.4$ mm s^{-1} and $\delta = 1.24$ mm s^{-1} at 12 K) is due to Fe(II) in the high-spin state. Such a component is typical for samples prepared by thermal decomposition of iron pentacarbonyl [24], and is probably due to left-overs of an intermediate iron–surfactant complex.

When measured at temperatures above 130 K the Mössbauer spectra show no magnetic splitting (see figure 2). This is due to fast superparamagnetic relaxation [29]. As the Fe–C particles are ferromagnetic the relaxation can be suppressed by applying a magnetic field. This was demonstrated in [29], and the mean magnetic moment of

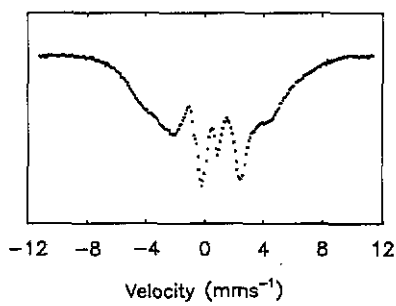

Figure 1. Mössbauer spectrum of sample A obtained at 12 K.

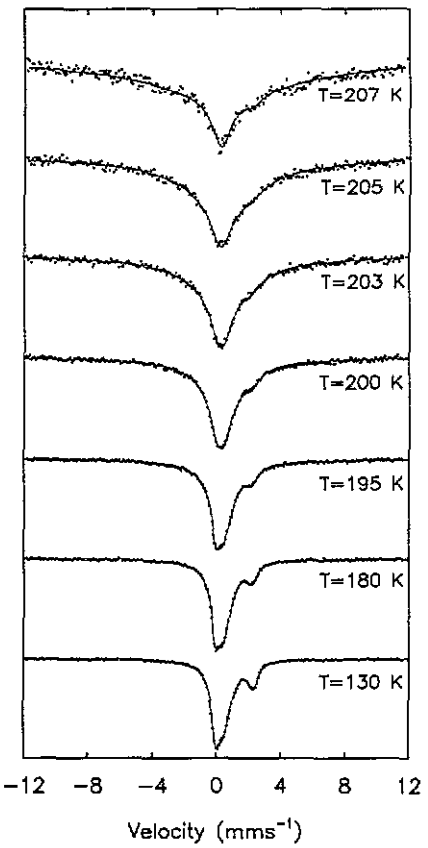

Figure 2. Mössbauer spectra of 3.3 nm amorphous iron–carbon particles in decalin (sample A). The spectra were obtained in order of increasing temperature, the decalin being crystalline during this series. The full curves in the figure are best-fit curves, where the fitting has been made in accordance with the model of Brownian oscillations.

the particles was estimated from the dependence of the induced hyperfine field on the applied magnetic field [30]. Assuming that the magnetic moment of the iron atoms in the particles is like that of an amorphous iron–carbon film with the same carbon content, and that the density of the particles is like that of Fe_3C, a mean particle size of 3.3 nm was estimated. This is in good agreement with the particle size estimated from electron micrographs [29].

All measurements to be discussed for sample A have been performed at temperatures above the blocking temperature—the temperature above which the superparamagnetic relaxation is so fast that the magnetic hyperfine splitting has collapsed. Therefore we can rule out magnetic relaxation effects as a cause of line broadening.

The Mössbauer spectra, shown in figure 2, were obtained in order of increasing temperature. The dominating component in the spectra is a broad singlet (δ = 0.40 mm s^{-1} at 130 K) arising from the amorphous iron–carbon phase. The Fe(II) doublet (ΔE_Q = 2.37 mm s^{-1}, δ = 1.13 mm s^{-1}) holds at 130 K about 20%

of the area. Spectra obtained at temperatures between 130 K and 180 K do not differ very much, but as the temperature is increased above 180 K one observes the appearence of a broad component in the spectrum. The width and relative area of this component increases with increasing temperature. The full curves in the spectra are best-fit curves, where the spectra have been fitted with an Fe(II) doublet, a single Lorentzian line having a line width equal to the minimum observed under the whole series (160 K) and a series of broader Lorentzians as given by (5). (Only the first five lines of the expansion have been included in the fitting routine.) The relative line widths and intensities have been constrained to fulfill the relations given in (5). The line widths of the broad components expressed in terms of the parameter $\hbar\alpha$ and the relative area of the narrow Lorentzian (A_0/A), inferred from the best-fit curves within the model of Brownian oscillations, are shown in figure 3. Figure 4 shows the variation of the area of the unbroadened peak (A_0) and the variation of the total area ($A = A_0 + A_{Fe(II)} + A_{broad}$) of the Mössbauer spectrum with temperature.

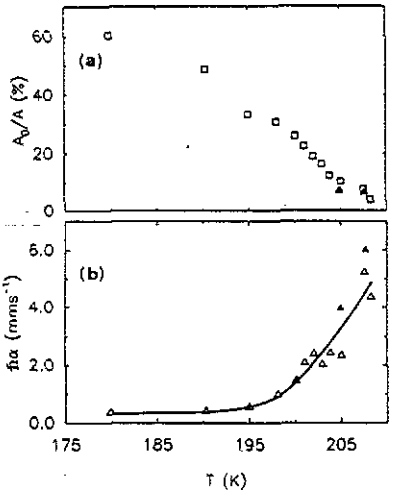

Figure 3. (a) The fraction of the total area (A_0/A, $A = A_{Fe(II)} + A_0 + A_{broad}$) found in the unbroadened elastic peak of sample A. The areas of the different components are evaluated from the computer fits. (b) The line broadening of sample A expressed by the parameter $\hbar\alpha$. The expression $\hbar\alpha$ is equal to the difference in line width between the unbroadened line and the first of the broad components. The full curve is a guide to the eye. Open and full symbols indicate that the corresponding spectra were obtained in velocity intervals of ± 12 mm s^{-1} and ± 24 mm s^{-1}, respectively.

In the fitting of the high-temperature spectra the isomer shift and the quadrupole splitting of the Fe(II) doublet have been constrained to follow an extrapolated low-temperature behaviour (where 'low temperature' is the temperature interval in which no broad components are observed). As no *a priori* assumptions can be made concerning the area ratio of the Fe(II) and the metallic component, this ratio has not been constrained in the fitting of the high-temperature spectra. The relative area of the Fe(II) doublet decreases with increasing temperature from about 15% at 180 K to about 5% at 205 K.

4.2. Sample B

The Mössbauer spectrum of sample B obtained at 12 K is shown in figure 5. The

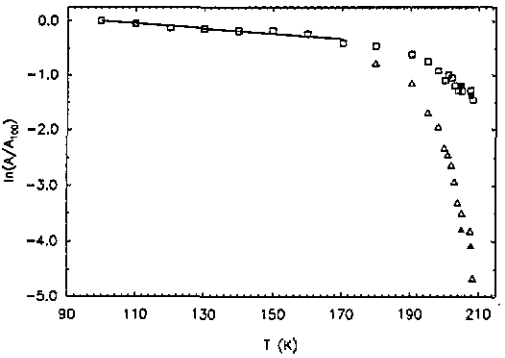

Figure 4. The natural logarithm of the area of the Mössbauer spectrum, relative to the area at 100 K, plotted versus temperature for sample A. The triangles are the areas of the unbroadened component and the squares are the total areas. The straight line is a best-fit line in the low-temperature region. Open and solid symbols indicate that the corresponding spectra were obtained in velocity intervals of ± 12 mm s^{-1} and ± 24 mm s^{-1}, respectively.

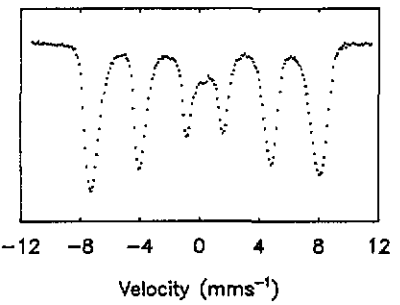

Figure 5. Mössbauer spectrum of sample B obtained at 12 K.

spectrum is magnetically split and has quite broad lines indicating a disordered structure. The mean hyperfine field is approximately 48 T, which is close to that reported for amorphous Fe_2O_3 [31, 32].

The particle size distribution obtained from electron micrographs of the sample is shown in figure 6. The mean particle size is estimated to be 6.8 nm.

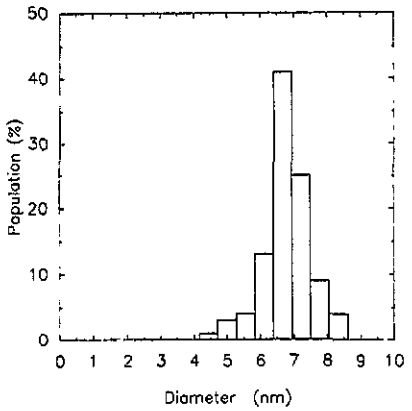

Figure 6. Particle size distribution of sample B estimated from electron micrographs.

When measured at higher temperatures the magnetic hyperfine splitting collapses due to fast superparamagnetic relaxation (figure 7). Contrarily to in the case of sample A, the relaxation cannot be suppressed by application of an external magnetic field. This implies that the particles have a very small, or no, resulting magnetic moment.

In figures 7 and 8 are shown Mössbauer spectra obtained at various temperatures

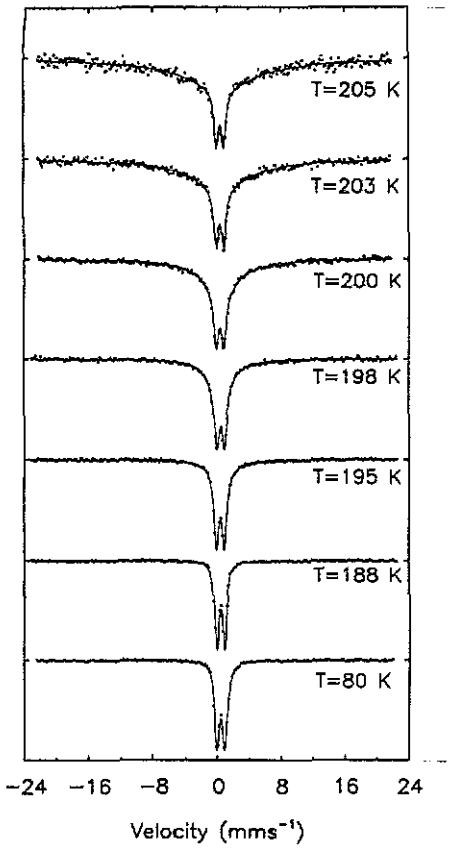

Figure 7. Mössbauer spectra of 6.8 nm iron oxide particles in decalin (sample B). The spectra have been obtained in order of increasing temperature. The decalin is crystalline during this series. The full curves are best-fit curves within the model of Brownian oscillations.

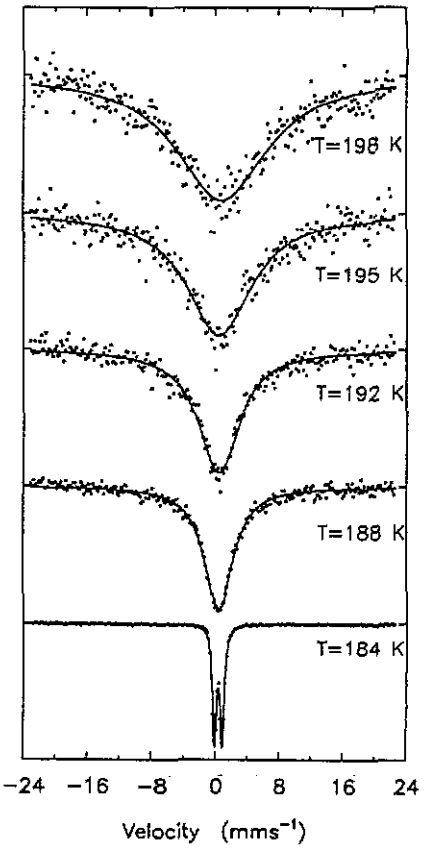

Figure 8. Mössbauer spectra of 6.8 nm iron oxide particles in decalin (sample B). The spectra have been obtained in order of decreasing temperature. Prior to the first measurement the samples have been heated to a temperature above the melting point of the carrier medium. The decalin is a supercooled liquid during this series. The full curves are best-fit curves with one quadrupole doublet.

in order of increasing and decreasing temperature, respectively. The spectra consist of an Fe(III) doublet with a quadrupole splitting of 0.98 mm s^{-1} and an isomer shift of 0.44 mm s^{-1} (at 122 K). In between the two series of measurements the sample has been heated to a temperature well above its melting point. Clearly the thermal history of the sample influences the Mössbauer spectra.

In figure 7 one sees the same tendency as in figure 2, namely that above a certain temperature (188 K) a broad component appears in the spectrum. The width and the relative area of this component increases with temperature. The full curves in figure 7 are best-fit curves using the model of Brownian oscillations—that is, fitting the spectra with a series of doublets with intensities and widths constrained to fulfil equation (5). (Only the first five doublets of the expansion have been included.) The difference in line width between consecutive Lorentzians ($\hbar\alpha$) as well as the relative area of the narrow Lorentzian ($A_0/(A_0 + A_{\text{broad}})$) determined from these fits are

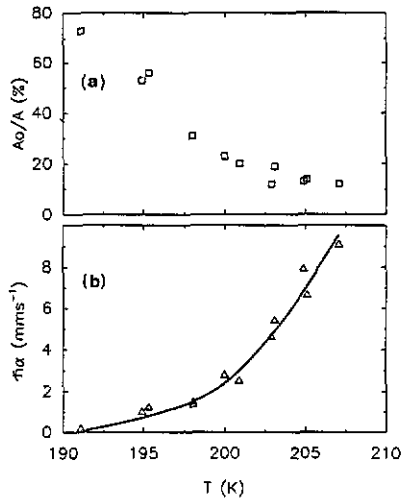

Figure 9. (a) The fraction of the total area $(A_0/(A_0+A_{broad}))$ found in the unbroadened elastic peak in the heating series of sample B. (b) The line widths of the broad Lorentzians expressed by the parameter $\hbar\alpha$ of the heating series of sample B. The full curve is a guide to the eye.

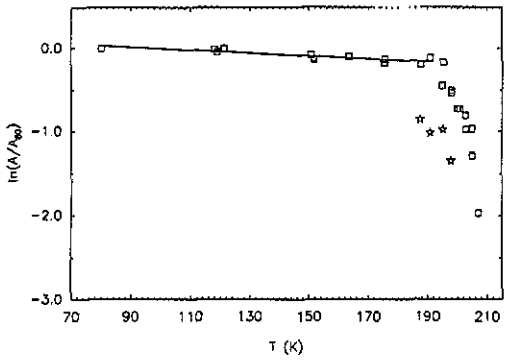

Figure 10. The natural logarithm of the area of the Mössbauer spectrum, relative to the area at 80 K, plotted versus temperature for sample B. The squares and stars are the total areas obtained in the heating and cooling series, respectively. The full curve is a best-fit straight line in the low-temperature region.

shown in figure 9. The variations of the total area of the Mössbauer spectrum with temperature are shown in figure 10 for both the heating and the cooling series.

The observed broadening in figures 2 and 7 cannot be explained as ordinary diffusion broadening. Both narrow and broad components are necessary to account for the change in line shape, as illustrated in figure 11 which shows a best-fit curve with only one quadrupole doublet (a) and the fit that results from fitting with the Brownian oscillator model (b). Clearly the one-doublet fit is inadequate. Figure 11 also shows the components of the fit in the Brownian oscillator model.

In figure 8, where spectra have beeen obtained in order of decreasing temperature, the picture is quite different. Here a strong broadening of the doublet is observed. The full curves are best-fit curves, where the fitting has been made with only one

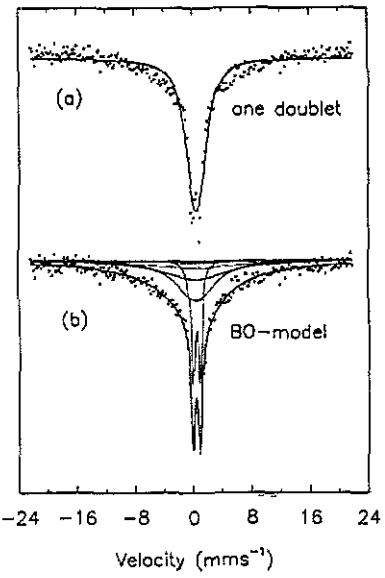

Figure 11. Comparisons of best-fit curves, of the Mössbauer spectrum of sample B at 203 K, with one quadrupole doublet (a) and with the Brownian oscillator model (b). The components of the fit are also shown.

doublet with Lorentzian line shapes, and clearly this gives quite adequate fits. This is in agreement with the Singwi–Sjölander theory of how Brownian motion influences the Mössbauer spectrum [1]. When the sample is cooled to 184 K the spectrum becomes identical to the spectrum obtained at the same temperature in the 'heating series'. This hysteresis is fully reproducible, and the explanation for the occurrence of hysteresis is that in the 'cooling series' the decalin is a supercooled liquid, whereas in the 'heating series' it is crystalline. This has been confirmed both by DTA measurements and by x-ray diffraction. The DTA measurements show a melting peak at 204 K when the sample has been cooled to 80 K before the start of the experiment, but no exothermic process is observed when the sample is only cooled to 170 K before the experiment (see figure 12) indicating that the decalin is a supercooled liquid in the latter case. The Debye–Scherrer x-ray pictures have sharp rings when the picture is taken at a sample temperature of 80 K, and no such sharp rings when the sample is heated to temperatures above the melting point of decalin, showing that the decalin is indeed crystalline at low temperatures.

5. Discussion

In both samples the natural logarithm of the area was found to decrease linearly with temperature in the low-temperature limit. This is what is expected for lattice vibrations when these are modelled with a Debye or an Einstein model [33]. The equivalent Debye temperatures (θ_D) extracted from the slope of the lines in figures 4 and 10 are 170 ± 15 K and 275 ± 50 K for the samples A and B, respectively.

The value for sample A is very low compared with, for example, the value for metallic iron ($\theta_D = 470$ K for α-iron [34]). This low equivalent Debye temperature

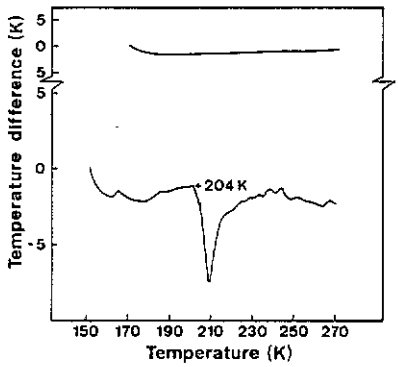

Figure 12. Results of DTA on a decalin-based ferrofluid. Prior to the measurement of the upper curve the sample was cooled to 170 K and prior to the measurement of the lower curve the sample was cooled to 80 K. The curves show the temperature difference between the sample and a reference, versus reference temperature, when the sample and reference are heated at a constant rate.

indicates that the mean-square displacement of the nuclei increases faster with temperature in these small iron–carbon particles than in bulk α-iron. This is probably an effect of the very small size of the particles, i.e. due to fast particle vibrations. Such an effect is well known from numerous studies of ultrafine particles [17, 34–36]. Another mechanism that might also lead to a lowering of the recoilless fraction in ultrafine particles, as compared to the bulk, is the existence of special vibrational surface modes [35, 37].

The equivalent Debye temperature value for sample B is quite close to reported values for maghemite (θ_D = 225 K [34]). Hence, finite-size effects seem not to influence the area variation at low temperatures for these larger particles.

For both samples a rapid decrease of the resonant area is observed in the temperature region where the broad lines appear in the spectrum. The model of Brownian oscillations shifts the area from the elastic peak to the broader quasi-elastic lines. This shift of area is indeed observed (figures 3 and 9), but also an overall loss is seen, which cannot be explained by the Brownian oscillator model. The loss of area could be due to very broad components lying outside the investigated velocity interval. To examine whether this is the case, we performed measurements in larger velocity intervals. Figure 13 shows Mössbauer spectra of sample B obtained in the velocity ranges ± 30 mm s^{-1} and ± 80 mm s^{-1}. The fitting parameters are the same, within uncertanties, in the two cases, i.e. the lost area is not regained by increasing the velocity window up to ± 80 mm s^{-1}.

The 'lost area' can be expressed in terms of an equivalent mean-square displacement. We therefore have to modify the expression for the total mean-square displacement given in the section 2. If we assume that the mode of motion leading to this extra mean-square displacement is uncorrelated with the low-temperature vibrations and the Brownian oscillations, then the total mean-square displacement can be written as [5]

$$\langle x_{\mathrm{tot}}^2 \rangle = \langle x_{\mathrm{v}}^2 \rangle + \langle x_{\mathrm{BO}}^2 \rangle + \langle x_{\mathrm{ve}}^2 \rangle \tag{7}$$

where $\langle x_{\mathrm{v}}^2 \rangle$ is the mean-square displacement of the low-temperature vibrations (internal lattice vibrations and/or particle oscillations), $\langle x_{\mathrm{BO}}^2 \rangle$ the mean-square displacement

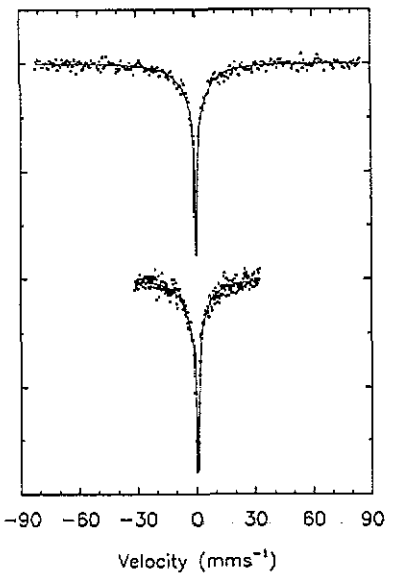

Figure 13. Mössbauer spectra of sample B, at 205 K, obtained in velocity intervals of ± 30 mm s^{-1} and ± 80 mm s^{-1}. The full curves are best-fit curves within the model of Brownian oscillations.

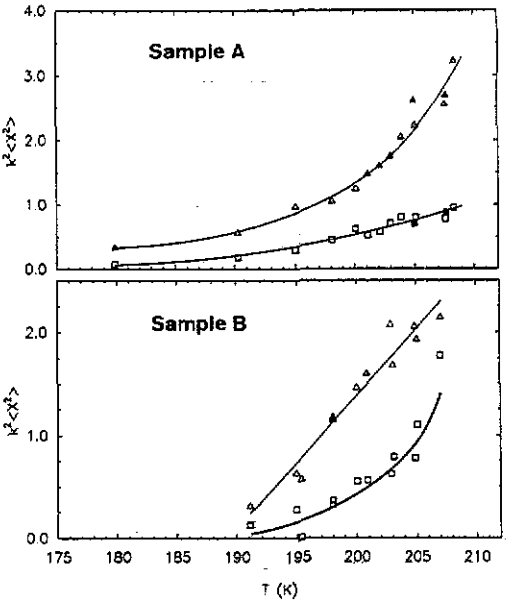

Figure 14. Mean-square displacements of the different modes of motion in sample A and sample B. The triangles are the mean-square displacements in the Brownian oscillations, and the squares are the necessary extra amplitudes needed to explain the overall loss of area. The full curves are guides to the eye. Open and full symbols indicate that the corresponding spectra were obtained in velocity intervals of ± 12 mm s^{-1} and ± 24 mm s^{-1}, respectively.

of the Brownian oscillations and $\langle x_{ve}^2 \rangle$ the extra vibrational amplitude added to explain the loss of area. The area in the narrow absorption line is proportional to $\exp(-k^2\langle x_{tot}^2 \rangle)$. The Brownian oscillations shift the area from the narrow absorption line to broader Lorentzians, but as these still lie within the velocity range of observation the total area of the Mössbauer spectrum is given by

$$A_{tot} \propto \exp(-k^2\langle x_v^2 \rangle) \exp(-k^2\langle x_{ve}^2 \rangle) . \tag{8}$$

In figure 14 the area variation of the spectra in figures 2 and 7 are expressed in terms of mean-square displacements.

The area of the spectra in the 'cooling series' of sample B (cf figure 8) are also considerably lower than expected from the extrapolated low-temperature behaviour (see figure 4). This loss of area has also been reported in other studies of particle diffusion [21].

When the decalin is crystalline (sample A and B, heating series) the changes in line shape are well expressed in the model of Brownian oscillations. The two parameters determining the line shape in the model are $\hbar\alpha$, which is the difference in line width between consecutive Lorentzians in the expansion, and $k^2\langle x_{BO}^2 \rangle$, which determines the relative area of the components. The temperature dependence of these parameters are shown in figures 3, 9 and 14.

The motional behaviour of the particles in a crystalline decalin matrix changes at a certain temperature (sample A: 180 K, sample B: 190 K). Below these temperatures the particles may perform fast oscillations which, especially for sample A, result in a rapid decrease of the area of the Mössbauer spectrum with temperature. Above these temperatures the particle motion is well described as Brownian oscillations. As the temperature is increased the Brownian oscillations become more and more dominating. The model accounts well for the line shape at all temperatures, but does not account for the observed loss of area.

The particles are coated with a monolayer of surfactant molecules, and the particles may be viewed as being mounted in the surrounding matrix with these 'molecular springs'. The motional behaviour of the particles depends on the characteristics of the coupling of the surfactant molecules to the matrix, and on the characteristics of the surfactant molecules themselves. The outermost molecular layer of the decalin matrix interacts with the surfactant molecules, and this layer may change its elastic properties, or even pre-melt, at temperatures below the bulk melting point. The fact that the change in the particle motion and the loss of area compared to the extrapolated low-temperature behaviour takes place somewhat below the melting point of the carrier medium supports this suggestion. At temperatures slightly below the melting point the thermal energy may be sufficient to break some of the weak bonds between the surfactant and matrix. This weakening of the bonding to the matrix will lead to an increase in the mean-square displacement of the particles, causing a loss of area compared with an extrapolated low-temperature behaviour. Such a mechanism can therefore explain the enhanced vibrational amplitude at these temperatures (expressed by $\langle x_{ve}^2 \rangle$).

One nice feature of the interpretation of the spectra in terms of the model of Brownian oscillations is that the observed features of co-existing narrow and broad lines and the increasing line width and weight of the broad components can be reproduced within this model. Only one correlation function is needed. One could argue that this might not be the case—the broad components could arise from diffusing particles and the narrow one from particles that are not allowed to diffuse. However, this would require a very broad distribution of diffusion constants, which seem unlikely due to the very narrow particle size distribution. Furthermore, we have seen no indication of particle clustering in the electron micrographs of the samples.

The dynamics of the colloidal system described in this work are, as seen by Mössbauer spectroscopy, very similar to what have been found for three otherwise quite different systems, namely for proteins [5, 6], for ultrafine particles in a polymeric network [15, 16], and for ions in a glycerol glass [18]. The similarity of the dynamics in the three latter systems have been ascribed to the common macromolecular nature of the systems [15]. The molecules (or molecular segments) in each of these systems are interacting via weak forces due to hydrogen bonds or van der Waals bonds. The particles in the system investigated in this work interact with the surrounding crystal in a similar way, i.e. via weak forces between the surfactant molecules and the decalin matrix. Thus it seems that the weak bonds between the molecules (or segments of molecules) is the common factor responsible for the similar dynamics of all these systems.

When the decalin is a supercooled liquid (sample B, cooling series) the temperature dependence of the line broadening (Δ) is found to be well described by an Arrhenius law (see figure 15). This reflects the temperature dependence of the

diffusion constant, as these two quantities are proportional [1]:

$$\Delta = 2\hbar k^2 D\,. \tag{9}$$

The activation energy is found to be 0.4 ± 0.04 eV. In a study of the particle dynamics in a suspension of 10 nm magnetite particles in a diester carrier Winkler *et al* [9] also found an Arrhenius-like temperature dependence of the line broadening (with an activation energy of 0.6 eV).

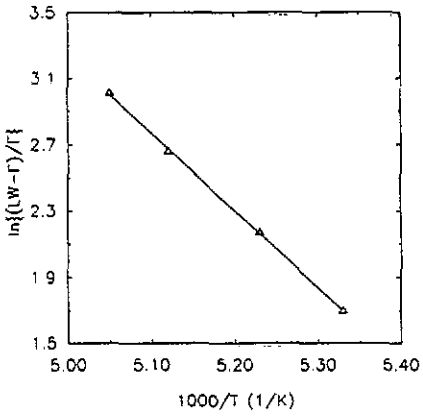

Figure 15. Arrhenius plot of the relative line broadening observed in the cooling series of sample B. LW is the observed line width and Γ the minimum line width observed in the whole series. The full line is the best fit of a straight line to the data points.

When the decalin is a supercooled liquid the line shape of the Mössbauer spectrum and the temperature dependence of the line width are in accordance with the theory of Singwi and Sjölander of how Brownian motion should influence the Mössbauer spectrum.

6. Conclusions

Ultrafine particles embedded in an organic crystalline matrix perform bound diffusive motion on a timescale in which the Mössbauer effect is sensitive, when the system is heated to temperatures close to the melting point of the matrix material.

The motion gives rise to very broad components in the Mössbauer spectrum, superimposed on the narrow elastic absorption line. This finding is very similar to what has been observed in studies of protein dynamics, and the spectral shape can be well accounted for by applying the model of overdamped harmonic oscillators, well known from the studies of protein dynamics [5, 6]. The motion of the nuclei are, as examined by Mössbauer spectroscopy, very similar in these otherwise very different systems.

The onset of the Brownian oscillations takes place at temperatures somewhat (≈ 15 K) below the melting temperature of the crystalline matrix, which indicates that the binding of the particles to the matrix softens in this temperature regime. This could be due to a 'pre-melting' in the immediate vicinity of the particles.

When the medium surrounding the particles is a supercooled liquid, a Lorentzian broadening of the absorption lines is observed in accordance with the theory of Singwi and Sjölander of how Brownian movement influences the Mössbauer spectrum. We would like to stress that the agreement between experiment and theory in this study is found in a very well-defined system in the sense that the particle size distribution is very narrow, and that magnetic relaxation effects do not contribute to the observed line broadening.

Acknowledgments

The studies were supported by the Danish Council for Technical Research. Michael Bentzon is gratefully acknowledged for performing electron microscopy and the Institute of Mineral Industry at the Technical University of Denmark is acknowledged for aid with the DTA.

References

[1] Singwi K S and Sjölander A 1960 *Phys. Rev.* **120** 1093
[2] Vogl G 1990 *Hyperfine Interact.* **53** 197
[3] Bauminger E R and Nowik I 1986 *Mössbauer spectroscopy* ed D P E Dickson and F J Berry (Cambridge: Cambridge University Press) p 219
[4] Bhide V G, Sundaram G, Bhasin H C and Bonchev T 1971 *Phys. Rev.* B **3** 673
[5] Parak F, Knapp E W and Kucheida D 1982 *J. Mol. Biol.* **161** 177
[6] Nowik I, Cohen S G, Bauminger E R and Ofer S 1983 *Phys. Rev. Lett.* **50** 152
[7] Mössbauer R L 1983 *Applications of the Mössbauer Effect* vol 1, ed Y M Kagan and I S Lyubutin (London: Gordon and Breach) p 1
[8] Kneller H and Kündig W 1975 *Solid State Commun.* **16** 253
[9] Winkler H, Heinrich H-J and Gerdau E 1976 *J. Physique Coll.* 37 C6 261
[10] Singh K P and Mullen J G 1972 *Phys. Rev.* A **6** 2354
[11] Heilmann I, Olsen B and Højgaard Jensen J 1974 *J. Phys. C: Solid State Phys.* **7** 4355
[12] Kordyuk S L, Lisichenko V I, Orlov O L, Polovina N N and Smoilovskii A N 1967 *Sov. Phys.-JETP* **25** 400
[13] Nowik I, Bauminger E R, Cohen S G and Ofer S 1985 *Phys. Rev.* A **31** 2291
[14] Parak F *Applications of the Mössbauer Effect* vol 1 ed Y M Kagan and I S Lyubtin (London: Gordon and Breach) p 113
[15] Nienhaus G U, Plachinda A S, Fisher M, Khromov V I, Parak F, Suzdalev I P and Goldanskii V I 1990 *Hyperfine Interact.* **56** 1471
[16] Plachinda A S, Sedov V E, Khromov V I, Bashkeev L V and Suzdalev I P 1990 *Hyperfine Interact.* **56** 1483
[17] Hayashi M, Gerkema E, van der Kraan A M and Tamura I 1990 *Phys. Rev.* B **42** 9771
[18] Parak F, Fisher M and Nienhaus G U 1989 *J. Mol. Liq.* **42** 145
[19] Craig P P and Sutin N 1963 *Phys. Rev. Lett.* **11** 460
[20] Bunbury D St P, Elliott J A, Hall H E and Williams J M 1963 *Phys. Lett.* **6** 34–6
[21] Abras A and Mullen J G 1972 *Phys. Rev.* A **6** 2343
[22] Elliott J A, Hall H E and Bunbury D St P 1966 *Proc. Phys. Soc.* **89** 595
[23] Knapp E W, Fisher S F and Parak F 1982 *J. Phys. Chem.* **86** 5042
[24] van Wonterghem J, Mørup S, Charles S W and Wells S 1988 *J. Colloid Interface Sci.* **121** 563
[25] Griffiths C H, O'Horo M P and Smith T W 1979 *J. Appl. Phys.* **50** 7108
[26] Hess P H and Parker,Jr. P H 1966 *J. Appl. Polym. Sci.* **10** 1915
[27] van Wonterghem J, Mørup S, Charles S W, Wells S and Villadsen J 1985 *Phys. Rev. Lett.* **55** 410
[28] Bentzon M D, van Wonterghem J, Mørup S, Thölen A and Koch C J W 1989 *Phil. Mag.* **60** 169
[29] Mørup S, Bødker F, van Wonterghem J, Madsen M B and Bentzon M D 1989 *Hyperfine Interact.* **51** 1071

[30] Mørup S 1984 *Mössbauer Spectroscopy Applied to Inorganic Chemistry* vol 2, ed G J Long (New York: Plenum) p 89
[31] Mørup S, Christensen B R, van Wonterghem J, Madsen M B, Charles S W and Wells S 1987 *J. Magn. Magn. Mater.* **67** 249
[32] van Diepen A M, Popma Th J A 1978 *Solid State Commun.* **27** 121
[33] Wertheim G K 1964 *Mössbauer Effect: Principles and Applications* (New York: Academic)
[34] Picone P J, Haneda K and Morrish A H 1982 *J. Phys. C: Solid State Phys.* **15** 317
[35] von Eynatten G and Bömmel H E 1977 *Appl. Phys.* **14** 415
[36] Viegers M P A and Trooster M 1977 *Phys. Rev.* B **15** 72
[37] Hayashi M, Tamura I, Fukano Y, Kanemaki S and Fujio Y 1980 *J. Phys. C: Solid State Phys.* **13** 681